CrossMark

ORIGINAL ARTICLE

Sorption of Cu²⁺ and Co²⁺ using zeolite synthesized from coal gangue: isotherm and kinetic studies

Xinwei Lu[1] · Dongqi Shi[1] · Jianlong Chen[1]

Abstract Adsorption of Cu²⁺ and Co²⁺ from aqueous solution using zeolite synthesized from coal gangue was examined at room temperature. Batch experiments were carried out to investigate the effects of contact time, initial ion concentration, and pH on the adsorption process. Under comparable conditions, the adsorption greatly depended on initial ion concentration and pH. Different isotherms were applied to describe equilibrium data, and the results turned out that adsorption data can be better fitted with Langmuir, Temkin, and Dubinin–Radushkevich models, indicating monolayer coverage of adsorption sites on the surface of zeolite NaX and a physical process for Co²⁺ and Cu²⁺ adsorption. Adsorption capacity calculated from Langmuir was 45.05 mg/g for Cu²⁺ and 44.53 mg/g for Co²⁺. The adsorption kinetic could be better described with the pseudo-second-order model, and the removal mechanism of Co²⁺ and Cu²⁺ by the synthesized zeolite NaX was governed by surface adsorption, film diffusion, and intra-particle diffusion. The work suggests that coal gangue-derived zeolite NaX can be used as an alternative economical adsorbent for metal ions removal.

Keywords Zeolite · Coal gangue · Adsorption · Metal ions · Isotherm and kinetic model

✉ Xinwei Lu
luxinwei@snnu.edu.cn

[1] Department of Environmental Science, School of Geography and Tourism, Shaanxi Normal University, Xi'an 710062, People's Republic of China

Introduction

Metal ions, non-biodegradable toxic inorganic pollutants (Bradl 2004), tend to accumulate in living organisms, causing various diseases and disorders (Bailey et al. 1999). Metal ions emerge from the course of mineral resources exploiting, metal smelting, and processing practices. As a kind of industrial resultant, metal ions have produced tremendous detriments to the ecological environment due to their non-biodegradation and long-term circulation within food chains. Gradually, chronic damage involved physiological and metabolic activities appears then health problems seem to be inevitable (Srividya and Mohanty 2009). Considering their ever-increasing negative impacts, skyrocketing attentions have been focused on finding out an efficient and green way to solve this environmental issue.

In recent years, removals of metal ions from water have been widely conducted (Dabrowski et al. 2004; Erdem et al. 2004). Many separation methods have been used for removal of metal ions from aqueous solution, including chemical precipitation, coagulation, solvent extraction, membrane filtration, ion exchange, reverse osmosis, chemical reduction, ultrafiltration, ionization, adsorption, biological treatment, and chelating resin (Hui et al. 2005; Baker et al. 2009; Padervand and Gholami 2013; El-Bahy and El-Bahy 2016; Petrovič and Simonič 2016; Iannazzo et al. 2017). However, most of these methods have significant disadvantages, such as the incomplete removal, high-energy requirements, and the production of toxic sludge (Petrovič and Simonič 2016; Iannazzo et al. 2017). Among those methods, adsorption has been proved to be one of the most feasible, simple, easily implemented, and highly efficient method for the removal of metal ions from polluted water (Kumar and Chawla 2014; Rahimi and

🖄 Springer

Mohaghegh 2016; Iannazzo et al. 2017). Some widely used adsorbents for metal ions include activated carbon, clay minerals, industrial solid wastes, orange peel, nanosized metal oxides (such as iron oxides, aluminum oxides, titanium oxides, and manganese oxides), and zeolites (Kumar and Chawla 2014; Rahimi and Mohaghegh 2016; Iannazzo et al. 2017). A green way of absorbing metal ions could be achieved by exploiting industrial derived and reproducible adsorbents, and it thus can contribute to further industrial applications.

Coal exploitation generally creates a large quantity of coal gangue as solid by-product. The accumulation of considerable coal gangue over the past years has resulted in serious environmental problems, e.g., land occupation and soil and groundwater pollution. Several alternatives, such as building materials, heat-insulating materials, and aluminum salt products, have been proposed and implemented to deal with it. In general, an adsorbent can be regarded as green if it needs little processing, abundant in nature, or a by-product even waste material from another industry (Bailey et al. 1999). Conversion of coal gangue to zeolite is one of the potential alternatives for handling the coal gangue as it has high content of silica and alumina, which are the basic components for zeolite formation. In general, there are two main methods (one-step and two-step methods) to synthesize zeolite with solid wastes as silica–alumina source (Qian and Li 2015). As for the application of removing metal ions from aqueous solution, zeolites were reported to exhibit high sorption capacity, sorption affinity, and cation exchange capacity for divalent sorbates (Apiratikul and Pavasant 2008; Rahimi and Mohaghegh 2016). According to our knowledge, however, scarce attempt has been made to convert coal gangue to zeolites (Zhang et al. 2008; Lei et al. 2009; Qian and Li 2015).

This work focused on Co^{2+} and Cu^{2+} removal from aqueous solution using zeolite NaX prepared from coal gangue as adsorbent. The adsorption influence factors such as initial ion concentration, pH, and contact time were investigated. Langmuir, Freundlich, Temkin, and Dubinin–Radushkevich isotherm models were used to describe the adsorption equilibrium data. Pseudo-first-order model, pseudo-second-order model, intra-particle model, and film diffusion model were employed to reveal the adsorption mechanism.

Materials and methods

Materials

Coal gangue, used as silicon and aluminum sources in this work, was collected from Baishui coal mine of Weibei area, China. It contains 45.14% SiO_2, 26.97% Al_2O_3, 0.32% MgO, 0.47% CaO, 1.21% Fe_2O_3, 1.02% K_2O, 0.21% Na_2O, 0.51% TiO_2, and 16.40% loss on ignition. Coal gangue primarily consists of kaolinite, quartz, and hematite. The mineral compositions and chemical components of coal gangue indicate that this kind of mining solid waste could be a promising resource for zeolite synthesis.

Other inorganic chemicals, such as copper nitrate $(Cu(NO_3)_2 \cdot 3H_2O)$, cobalt nitrate $(Co(NO_3)_2 \cdot 6H_2O)$, sodium hydroxide (NaOH), nitric acid (HNO_3), and hydrochloric acid (HCl) are all analytic-grade reagents. Copper nitrate and cobalt nitrate were purchased from Jinshanting chemical reagent plant of Shanghai, while sodium hydroxide, nitric acid, and hydrochloric acid were bought from Tianjin chemical reagent plant. Stock solutions (1000 mg/L) were prepared by dissolving accurate mass of $Co(NO_3)_2 \cdot 6H_2O$ and $Cu(NO_3)_2 \cdot 3H_2O$ into 1000 mL deionized water. Desired concentrations were obtained by diluting the stock solution with deionized water.

Preparation of zeolite

Zeolite NaX was synthesized from coal gangue via hydrothermal treatment after alkali fusion. The milled coal gangue sample was calcinated at 800 °C for 3 h and then mixed with NaOH at an optimal weight ratio of nearly 1.2:1. The resultant was then roasted holding by a nickel crucible at 600 °C for 3 h in a muffle furnace. The alkali-fused product was milled and transferred into a 100-mL-volume beaker, aging for 6 h at a constant liquid/solid ratio at 8 mL/g. The aged product was transferred into a 100-mL-volume polytetrafluoroethylene reactor and crystallized at 110 °C for 12 h in an oven (Chen and Lu 2017). Then, the product was separated from the mixture through vacuum filtration with deionized water to removal excess sodium hydroxide until the pH reaching 9–10 and dried at 105 °C before storing in a desiccator.

Characterization of zeolite

The synthesized products were characterized with X-ray diffraction (XRD) and scanning electron microscope (SEM). XRD pattern was obtained using a Rigaku D/Max2550VB+/PC X-Ray diffractometer with Cu Kα ($\lambda = 0.154$ nm) radiation operating at 40 kV, 100 mA, scan rate of 4°/min, and step width of 0.02°. The surface morphology and microstructure of the synthesized zeolite products were characterized by a Hitachi S-3400N scanning electron microscope (SEM) and energy-dispersive X-ray spectrometer (EDXS) combined instrument. The surface area analyzer, JW-BK132F, was

applied to determine surface area using BET technique based on adsorption–desorption characteristics of N_2 gas on the sample at 77 K. The micropore size distribution was determined by Barrett–Joyner–Halenda (BJH) method using the adsorption branch (Huang et al. 2010). The point of zero charge (pH_{pzc}) was determined with JS94H2 Zeta Meter electrophoresis by measuring the surface charge of zeolite NaX in deionized water at different pH.

Batch sorption experiment

Effect of initial pH

The initial pH of the aqueous solution is a crucial controlling parameter during the adsorption process. To clarify the influence of initial pH of solution, batch sorption experiments were carried out at different initial pH solution (2.0–6.0), adjusted by 0.1 mol/L HNO_3 or NaOH solution. In this study, 0.2 g zeolite NaX was, respectively, added into 100 mL Cu^{2+} solution (100 mg/L) and 100 mL Co^{2+} solution (100 mg/L), agitated at 300 rpm for 120 min at ambient temperature (27 °C). The equilibrium mixture was filtered with a 0.45-μm filter membrane, and the residual Cu^{2+} and Co^{2+} concentrations in the solution were measured by inductively coupled plasma atomic emission spectroscopy (ICP-AES, Spectro Arcos).

Effect of initial ion concentration

Parallel experiments were conducted to reveal the influence of the initial ion concentration on adsorption. In this study, the initial ion concentration varied from 10 to 200 mg/L, while other experimental conditions such as initial pH (4.0) of solution, zeolite NaX dose (0.2 g), experimental temperature (room temperature, 27 °C), stirring time (120 min), and rotational speed (300 rpm) were fixed through the process. Graph of adsorption capacity versus initial ion concentration was plotted to determine the optimum initial ion concentration.

Adsorption kinetic experiment

Kinetic studies were conducted in 250-mL conical flasks. In total, 0.2 g dried zeolite NaX was thoroughly mixed with 100 mL metal ion solution at five different initial ion concentrations (10, 20, 50, 100 and 200 mg/L), and the pH of the solution was adjusted to 4.0 using 0.1 mol/L HNO_3 or 0.1 mol/L NaOH. The suspension was stirred at room temperature (27 °C) under a rate of 300 rpm. Samples of 0.5 mL solution were extracted from the conical flasks at the given time (0, 5, 10, 20, 40, 60, 80, 100, and 120 min).

The total extraction volume was no more than 5% of the stock ion solution. The extracted solutions were filtered with 0.45-μm filter membrane. The ion concentration in the solution was determined by ICP-AES.

Metal ions uptake

The removal efficiency (R, %) and the amount of ion adsorbed at time t (q_t, mg/g) and at equilibrium (q_e, mg/g) were calculated using the following equations, respectively (Srividya and Mohanty 2009; Zhao et al. 2010).

$$R = \frac{(C_0 - C_e) \times 100}{C_0} \tag{1}$$

$$q_t = \frac{(C_0 - C_t) \times V}{M} \tag{2}$$

$$q_e = \frac{(C_0 - C_e) \times V}{M} \tag{3}$$

where C_0, C_t, and C_e (mg/L) represent the ion concentrations at initial, t time, and equilibrium, respectively. V (L) is the volume of ion solution, and M (g) is the mass of zeolite NaX.

Results and discussion

Characterization of zeolite

The crystalline phase of the synthesized product was characterized by XRD (Fig. 1). Diffractogram of the synthesized product matches the reference peaks of zeolite NaX (PDF: 38-0237) well. Comparison of the characteristic peak confirmed the conversion of coal gangue into zeolite NaX. Surface morphology was checked by SEM (Fig. 2). Octahedron crystalline structure of the synthesized
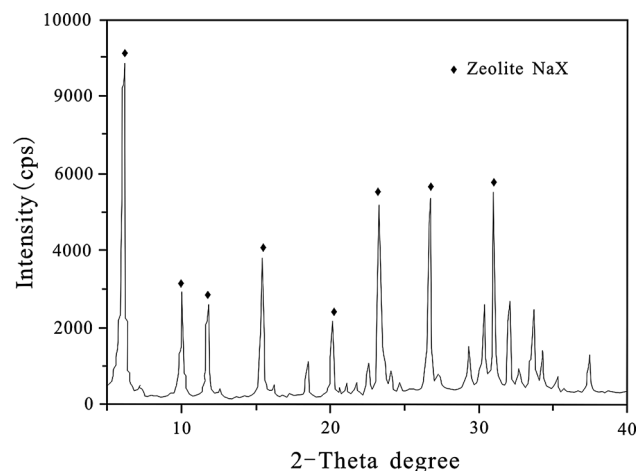

Fig. 1 X-ray diffraction pattern of zeolite synthesized from coal gangue
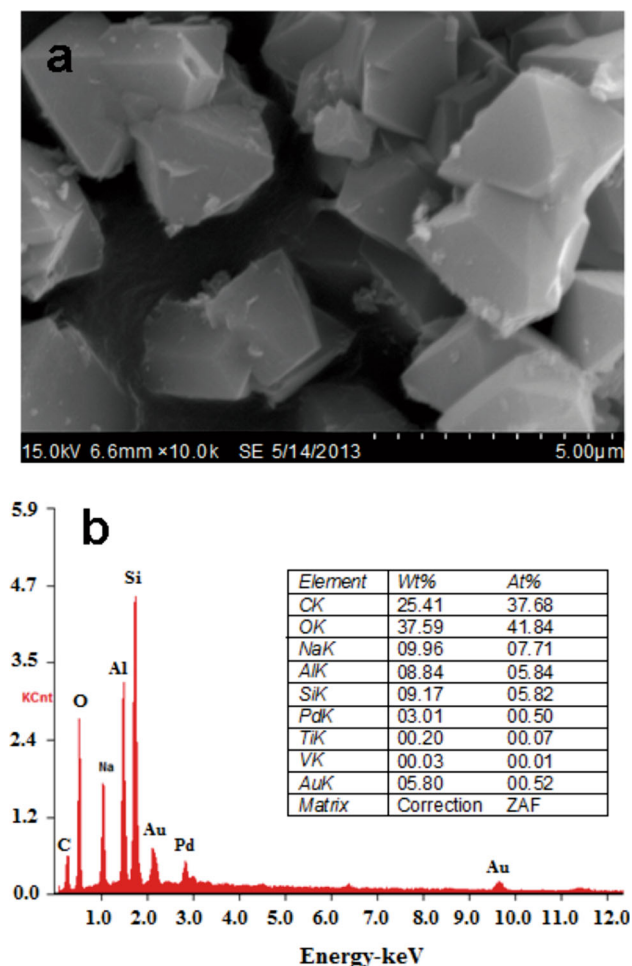
Fig. 2 Scanning electron microscopy image (**a**) and energy-dispersive X-ray spectrometer spectrum with element content (**b**) of zeolite synthesized from coal gangue

zeolite NaX particles can be clearly observed (Fig. 2a), which further indicates that the coal gangue was successfully transformed to target product. EDXS analysis result (Fig. 2b) suggests a molar ratio of SiO_2/Al_2O_3 of 2.1. The specific surface area and the micropore total volume of the synthesized zeolite NaX are 676.02 m^2/g and 0.263 cm^3/g, respectively, indicating that the synthesized zeolite NaX is a potential effective adsorbent. It has a wide range of pore dimension within micropore range (<2 nm), which is possible to separate different metal ions from polluted wastewater.

The point of zero charge (pH_{PZC}) of an adsorbent is crucial to choose the optimum pH for the adsorption study, as well as to understand the adsorption mechanism (Argun 2008; Göde et al. 2010). The pH_{PZC} of the synthesized zeolite NaX is 3.8. The surface charge remains positive when the pH below 3.8 and negatively charged once the pH beyond that point which is favorable for adsorption of positively charged metal ions.

Effect of initial pH

The ionization degree of the adsorbate and the surface property of the sorbent as well as metal ion species were strongly affected by the aqueous solution pH (Lin and Yang 2002; Rivera-Utrilla and Sánchez-Polo 2003). It is necessary to be viewed as an important factor that can greatly affect the removal efficiency in an adsorption system. Hui et al. (2005) pointed out that the ionization of surface hydroxyl groups (Si–OH and Al–OH) can change when zeolite surface exposed to aqueous solution. Covarrubias et al. (2005) stated that positively charged metal ions may react with hydroxyl in aqueous and the zeolite surface may in turn influence the surface charge and finally changed the removal efficiency. Batch adsorption experiments concerning the removal efficiency as the function of initial solution pH (2.0, 3.0, 4.0, 5.0, 6.0) were conducted. pH was adjusted before adding zeolite NaX. Higher initial pH was excluded in the case of precipitation, which could lead to a sharp increase in removal efficiency (Hui et al. 2005). The experiments show that the adsorption amount of Co^{2+} and Cu^{2+} onto zeolite NaX increases once the pH rises up from 2.0 to 6.0, especially when pH varied from 2.0 to 4.0. The removal efficiency increases slowly when pH changed from 4.0 to 6.0. This can be elucidated by the balance effect involving the surface charge and solution chemistry as well as the zeolite structure (Moghadam et al. 2013). Zeolite consists of body part, negative charged aluminosilicate frame structure, and balanced by positively charged exchangeable alkali ions (Na^+, K^+) to keep an electric neutrality state. Exposed to highly acid environment (lower than the isoelectric point of the zeolite NaX) leads to a positively charged zeolite NaX surface due to an exchange reaction between the hydrogen ion and alkali ions. At lower pH, the concentration of H_3O^+ is much higher than that of metal ions, and hence the former metal ions occupy the binding sites on the zeolite surface, resulting in a lower removal efficiency. On the other hand, Cu^{2+} and Co^{2+} can complex with hydroxyl when pH > 4.0 and a steric hindrance effect appears, and then metal ions cannot pass through the pore which lead to a relative slow increase in Cu^{2+} and Co^{2+} removal efficiency.

Effect of initial metal ion concentration

Metal ions can be adsorbed onto certain amount of zeolite. In that way, attentions should be paid to investigate the influence of initial ion concentration on metal ions removal. The relationship between sorption capacity and the initial concentration (ranged from 10 to 200 mg/L) is shown in Fig. 3. As it can be observed clearly, a rise of initial ion concentration contributes to an increase in metal
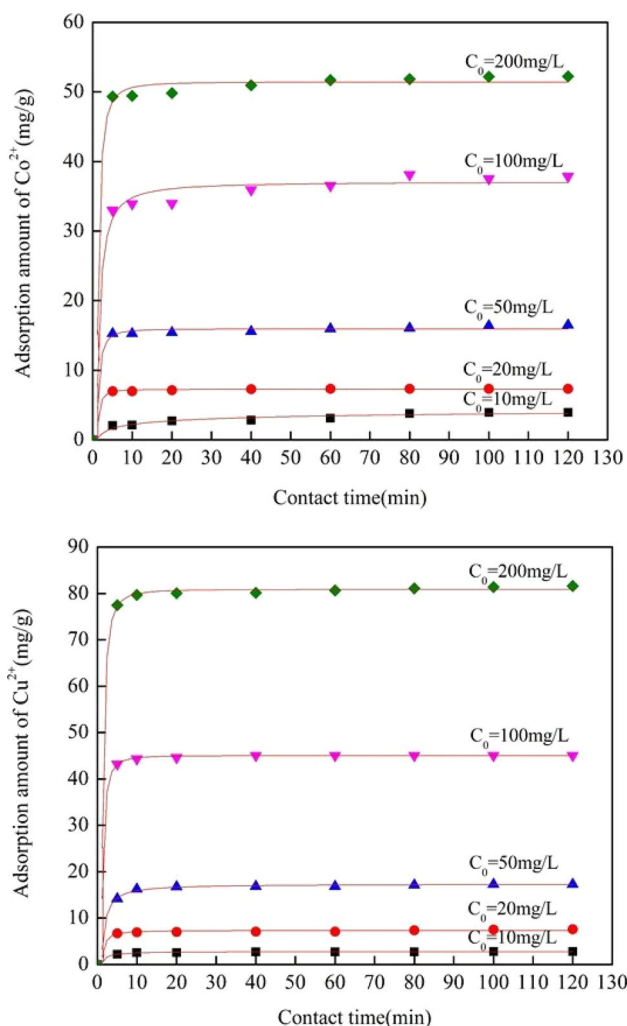
Fig. 3 Relationship between contact time and adsorption capacity at different initial metal ion concentrations

ion adsorption capacity to a certain point and then reaches a climax, which could be explained by the saturation of adsorption active sites. Additionally, the figure also demonstrates that metal ions were almost removed within the first 40 min though relative longer time was needed to reach equilibrium at higher initial metal concentration when compared with lower ones for both of the cases. Sharp adsorption at the beginning can be ascribed to the greater metal ion concentration difference during the first several minutes, which exhibits stronger adsorption driver force.

Kinetic studies

Further information about the reaction route and mechanism in an adsorption system can be revealed by the adsorption kinetic studies. Moreover, deep insights into the solute adsorption can be obtained through the analysis of

the adsorption experiment data using proper sorption kinetic models (Ho and McKay 1999). It can also help to determine the remnant time needs to reach equilibrium at the solid–solution interface. So far, several sorption kinetic models have been proposed to understand the adsorption characteristics. Among them, the most widely used were pseudo-first-order equation, pseudo-second-order equation, intra-particle diffusion model, and liquid film diffusion model.

The pseudo-first-order adsorption kinetic model used to describe adsorption in a liquid–solid system can be expressed as

$$\log(q_e - q_t) = \log(q_e) - \frac{K_1}{2.303}t \tag{4}$$

where q_e (mg/g) and q_t (mg/g) refer to the amount of adsorbed metal ions on zeolite NaX at equilibrium and time t, respectively. t is the reaction time (min) and K_1 (min^{-1}) represents the pseudo-first-order adsorption rate constant. K_1 and q_e can be obtained from the slope and intercept in log (q_e-q_t) against t plot, respectively.

The pseudo-second-order kinetic model is expressed as

$$\frac{t}{q_t} = \frac{1}{K_2 q_e^2} + \frac{t}{q_e} \tag{5}$$

where q_e (mg/g) and q_t (mg/g) mean the amount of adsorbed metal ions on zeolite NaX at equilibrium and at time t, respectively. K_2 (g/(mg·min)) is the pseudo-second-order rate constant. K_2 and q_e can be known through the graph of t/q_t versus t.

To calculate the above rate constants, the pseudo-first-order equation and pseudo-second-order equation were employed to fit sorption data of Co^{2+} and Cu^{2+} (under five different concentrations) with a fixed adsorbent dose. The values of the reaction rate constants and correlation coefficients are listed in Table 1. A comparison between the pseudo-first-order and pseudo-second-order kinetic rate constants suggests that Co^{2+} and Cu^{2+} adsorption by zeolite NaX closely follows the pseudo-second-order kinetic rather than the other one. This is clearly exhibited in Table 1, since the values of q_e obtained from pseudo-second-order kinetic equation was found to be closer to the experimental q_e value, whereas pseudo-first-order q_e value did not agree with the experimental q_e.

The intra-particle diffusion model is represented as

$$q_t = K_{id}t^{\frac{1}{2}} + C \tag{6}$$

where K_{id} (mg/(g min$^{-1/2}$)) is the intra-particle diffusion rate constant. q_t is the amount of metal ions adsorbed at time t and C (mg/g) is a constant proportional to the thickness of boundary layer (Arivoli and Ravichandran 2013). Applying the intra-particle diffusion model to the

Table 1 Sorption kinetic parameters

Concentration (mg/L)	Metal ions	$q_{e,\ exp}$ (mg/g)	Pseudo-first-order kinetic model			Pseudo-second-order kinetic model		
			$q_{e,\ cal}$ (mg/g)	K_1 (min^{-1})	R^2	$q_{e,\ cal}$ (mg/g)	K_2 (g/mg/min)	R^2
10	Co^{2+}	5.10	4.02	0.026	0.906	5.12	0.2	0.9677
	Cu^{2+}	3.14	0.87	0.017	0.881	3.16	0.12	0.9851
20	Co^{2+}	7.55	0.72	0.021	0.837	7.51	0.15	0.9996
	Cu^{2+}	7.88	1.82	0.017	0.73	7.89	0.11	0.9999
50	Co^{2+}	18.05	1.14	0.015	0.779	18.07	0.016	0.9966
	Cu^{2+}	20.85	3.3	0.014	0.181	19.45	0.06	0.9731
100	Co^{2+}	42.34	10.13	0.015	0.619	42.37	0.0099	0.9993
	Cu^{2+}	45.76	2.34	0.01	0.543	45.77	0.046	0.9997
200	Co^{2+}	53.85	7.72	0.0083	0.744	53.82	0.0087	0.9997
	Cu^{2+}	85.60	8.19	0.01	0.625	85.4	0.007	0.9982

$q_{e,\ cal}$ represents the amount of metal ions adsorbed on the zeolite by modeling calculation at equilibrium

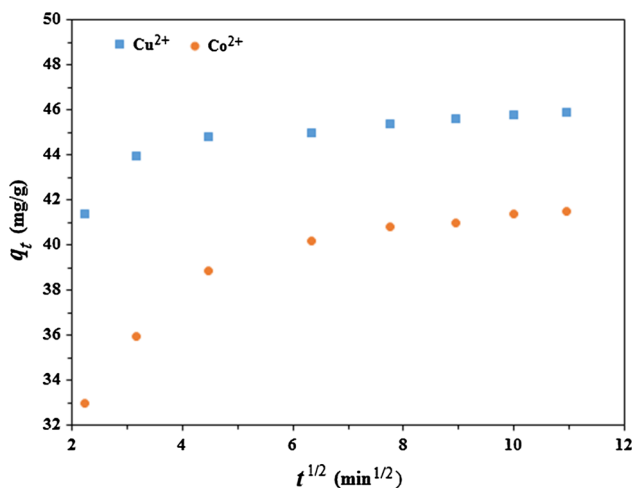$q_{e,\ exp}$ represents the experimental amount of metal ions adsorbed on the zeolite

Fig. 4 Intra-particle diffusion model for Cu^{2+} and Co^{2+} adsorbed onto zeolite synthesized from coal gangue

Fig. 5 Film diffusion model plot graphs for Cu^{2+} and Co^{2+} adsorbed onto zeolite synthesized from coal gangue

experimental data of Co^{2+} and Cu^{2+} adsorption, the fitting plot did not give straight lines to pass through the origin (Fig. 4). This may indicate that the mechanism of removal of Co^{2+} and Cu^{2+} by the synthesized zeolite NaX is complex, and the surface adsorption as well as intra-particle diffusion contributes to the rate-determining step (Salam 2013; Thamilarasu and Karunakaran 2013).

The liquid film diffusion is another kinetic model that assumes the flow of the adsorbate molecules through a liquid film surrounding the solid adsorbent is the slowest step in an adsorption process and it thus determines kinetic of the process (Salam 2013). The liquid film diffusion model is given by the following equation (Salam 2013)
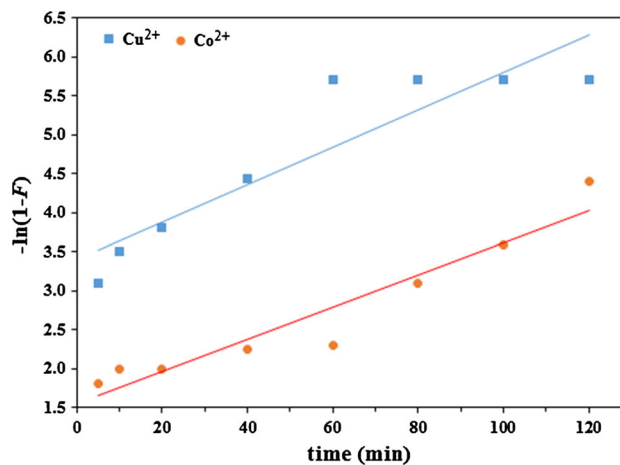
$$\ln(1 - F) = -K_{fd} \times t \qquad (7)$$

where $F = q_t/q_e$, the proportion of equilibrium achievement. K_{fd} (min^{-1}) is the film diffusion rate coefficient. A linear plot of $-\ln(1-F)$ versus t with zero intercept suggests that the kinetic of the adsorption process is controlled by diffusion process when passing through the liquid film. The liquid film diffusion model fitting plot did not cover all the experimental data points well and did not provide a straight line through the origin (Fig. 5). It indicates that the liquid film diffusion model was not the only determining step (Salam 2013).

Adsorption isotherm

The adsorption isotherm is the relationship between equilibrium concentration of the solute in the solution and

quantity of the adsorbate adsorbed by sorbent at constant temperature (Yuan et al. 2013). In the study, the experimental adsorption data were fitted with the most widely used isotherm models, that is, Langmuir, Freundlich, Temkin, and Dubinin–Radushkevich isotherm models (Erdem et al. 2004; Srividya and Mohanty 2009; Göde et al. 2010; Abdelnaeim et al. 2016; Chaudhry et al. 2017a, b).

The Langmuir model is based on the assumption that the uptake of metal ions occurs on a homogeneous surface by monolayer adsorption without any interaction between adsorbed ions (Srividya and Mohanty 2009; Abdelnaeim et al. 2016). The model further hypothesizes that the energy is same for all the active adsorption sites. The Langmuir isotherm model represents the equilibrium distribution of metal ions between the solid and liquid phases. The linear form of Langmuir equation is given as (Zhao et al. 2010; Arivoli and Ravichandran 2013)

$$\frac{C_e}{q_e} = \frac{1}{bq_m} + \frac{C_e}{q_m} \tag{8}$$

where C_e (mg/L) is the equilibrium concentration of metal ion in solution. q_e (mg/g) is the amount of metal ion adsorbed at equilibrium. q_m (mg/g) is the maximum metal ion uptake per unit mass of the adsorbent, which relates to adsorption capacity. b is the Langmuir constant (L/mg) which relates to the adsorption rate. The q_m and b can be determined from C_e/q_e versus the C_e plot which gives a straight line of slope $1/q_m$ and intercept $1/(bq_m)$. According to the Langmuir model, the maximum adsorption capacity of zeolite NaX is 44.53 mg/g for Co^{2+} and 45.05 mg/g for Cu^{2+} (Table 2).

The essential characteristics of Langmuir adsorption isotherm can be explained in terms of dimensionless constant called separation factor or equilibrium parameter, R_L ($R_L = 1/(1 + bC_0)$), where b is the Langmuir constant (L/mg) and C_0 is the initial concentration of metal ions. Four adsorption types were categorized according to the value of separation factor R_L (Arivoli and Ravichandran 2013): (1) favorable adsorption, $0 < R_L < 1$; (2) unfavorable adsorption, $R_L > 1$; (3) linear adsorption, $R_L = 1$ and (4) irreversible adsorption, $R_L = 0$. R_L is a positive number whose magnitude determines the feasibility of the adsorption process (Srividya and Mohanty 2009). The values of R_L for

Co^{2+} and Cu^{2+} adsorption on the synthesized zeolite NaX are all between 0 and 1, indicating that the synthesized zeolite NaX is an appropriate adsorbent for Co^{2+} and Cu^{2+}.

The Freundlich isotherm is the most frequently used to describe the adsorption of inorganic and organic components in solution (Hui et al. 2005). This fairly satisfactory empirical isotherm can be applied to a non-ideal sorption that involves heterogeneous sorption, and it is expressed as

$$\log q_e = \log K_F + \frac{1}{n} \log C_e \tag{9}$$

where C_e (mg/L) is the equilibrium concentration. K_F (mg/g(L/mg)$^{1/n}$) is roughly an indicator of the adsorption capacity and $1/n$ is the adsorption intensity of metal ion on the synthesized zeolite NaX. The magnitude of the exponent $1/n$ gives an indication of the favorability of adsorption. By plotting $\log q_e$ versus $\log C_e$, values of K_F and $1/n$ can be calculated from the slope and intercept of the plot. Table 2 shows that the $1/n$ values for Co^{2+} and Cu^{2+} are between 0 and 1, implying a favorable adsorption (Abdelnaeim et al. 2016).

Temkin isotherm is based on the assumption that the heat of adsorption of all molecules in the layer decrease linearly with the coverage of adsorbent surface. The isotherm is applicable for adsorption on heterogeneous solid adsorbent surface and liquid adsorbate. The linearized mathematical form of Temkin isotherm is (Abdelnaeim et al. 2016; Chaudhry et al. 2017a, b)

$$q_e = \frac{RT}{b_T} \ln A_T + \frac{RT}{b_T} \ln C_e \tag{10}$$

where C_e (mg/L) is the equilibrium concentration; A_T (L/mg) and b_T (kJ/mol) are Temkin constants related to equilibrium binding constant (L/mol) which is related to the maximum binding energy and heat of adsorption, respectively; R is the gas constant; T (K) is the temperature. The values of A_T and b_T for Co^{2+} and Cu^{2+} were calculated from the slope and intercept of the plots q_e versus $\ln C_e$ plots, and the results are given in Table 2. The regression coefficient values for Co^{2+} (0.998) and Cu^{2+} (0.996) indicate that the adsorption data were well fitted to Temkin isotherm model. Table 2 shows that the Temkin constant b_T related to heat of adsorption for Co^{2+} and Cu^{2+} is 0.261 and 0.264 kJ/mol, respectively. It has been reported that

Table 2 Parameters of different isotherms for Co^{2+} and Cu^{2+} adsorption onto zeolite synthesized from coal gangue

Metal ions	Langmuir			Freundlich			Temkin			Dubinin–Radushkevich		
	q_m mg/g	b L/mg	R^2	K_F mg/g(L/mg)$^{1/n}$	$1/n$	R^2	A_T L/g	b_T kJ/mol	R^2	q_s mg/g	k_{ad}	R^2
Co^{2+}	44.53	0.039	1.0	0.32	0.43	0.798	0.392	0.261	0.998	19.94	7E−06	0.996
Cu^{2+}	45.05	0.037	0.987	0.77	0.36	0.824	0.364	0.264	0.996	19.37	8E−06	0.994

the typical range of bonding energy for ion-exchange mechanism is 8–16 kJ/mol (Chaudhry et al. 2017b), and the low values in this study indicate a weak interaction between metal ions (Co^{2+} and Cu^{2+}) and the synthesized zeolite NaX (Chaudhry et al. 2017b). These results complemented Langmuir and Freundlich isotherm results.

Dubinin–Radushkevich isotherm model is applied to determine the nature of sorption process and the mean energy of sorption (Abdelnaeim et al. 2016). The linear form of Dubinin–Radushkevich isotherm is represented as (Abdelnaeim et al. 2016; Chaudhry et al. 2017a, b)

$$\ln q_e = \ln q_s - k_{ad}\varepsilon^2 \tag{11}$$

where k_{ad} is the Dubinin–Radushkevich constant related to mean free energy of adsorption (mol^2/kJ^2); q_s is theoretical Dubinin–Radushkevich monolayer saturation adsorption capacity (mg/g), and ε is Polanyi potential which is equal to $RT\ln(1 + 1/C_e)$. R and T are gas constant and temperature in Kelvin scale, respectively. The slope and intercept of the straight line plot of $\ln q_e$ versus ε^2 gave k_{ad} and q_s. The mean free energy of sorption can be calculated using the following equation

$$E = 1/\sqrt{2k_{da}} \tag{12}$$

If the value of E is between 8 and 16 kJ/mol, the adsorption process proceeds by ion exchange or chemisorption, and if the value of E less than 8 kJ/mol, the adsorption process is of a physical nature (Abdelnaeim et al. 2016). The values of E for Co^{2+} and Cu^{2+} are <8 kJ/mol, implying the adsorption of Co^{2+} and Cu^{2+} on the synthesized zeolite NaX is a physical process.

The correlation coefficients demonstrate that Langmuir, Temkin, and Dubinin–Radushkevich models adequately fitted the data for Co^{2+} and Cu^{2+} adsorption (Table 2). Such an observation gives a suggestion of monolayer adsorption of metal ions on the surface which means monolayer coverage of adsorption sites distribution (Kumar and Chawla 2014). Furthermore, adsorption capacity of Cu^{2+} and Co^{2+} calculated from Langmuir model were compared with the similar adsorbents (Erdem et al. 2004; Hui et al. 2005; Apiratikul and Pavasant 2008) in Table 3, from which we can know that the synthesized zeolite NaX has the relative strong adsorption capacity in removing heavy metal ions. On the other hand, the adsorption capacity order determined from Fig. 3 is $Co^{2+} < Cu^{2+}$.

Several factors, such as zeolite framework and hydrated radius sizes of the metal ions may lead to such a contradiction. From the point of the structure, coal gangue-derived zeolite NaX has a wide range distribution of effective pore diameter (6.6 Å, 7.4 Å and 8.4 Å)(Chen and Lu 2017). A specific structure zeolite can play as a retainer for the separation of metal ions that have different hydrated radius. If the size of the metal hydrated radius is greater, compared with the adsorbent, it cannot pass through it. In fact, the hydrated radius of Co^{2+} (4.23 Å) is higher than Cu^{2+} (4.04 Å)(Tansel et al. 2006), which can elucidate the adsorption sequence in our experiment, namely, $Co^{2+} < Cu^{2+}$. According to the study (Xu et al. 2010), the hydrogen may replace the exchangeable alkali ions (Na^+) that exist within the structure, leading to a raise of solution pH. The calculated beginning precipitation pH concerns Co^{2+} and Cu^{2+} is 7.94 and 5.74 under the adsorption condition, respectively. Turan et al. (2005) argued that the abated metal ion concentration equals to adsorption plus precipitation in a zeolite adsorption system. Quicker precipitation happens to Cu^{2+} rather than Co^{2+}, which contributes to faster precipitation of Cu^{2+} and higher adsorption capacity under experimental condition. Furthermore, we propose that adsorption is a process depends on the variety of adsorbents as well as experiment conditions.

Table 3 Comparison of the Langmuir constants for Cu^{2+} and Co^{2+} adsorption onto adsorbents

Adsorbent	Adsorbate	q_m (mg/g)	References
Coal fly-ash-derived zeolite NaX	Cu^{2+}	90.88	Apiratikul and Pavasant (2008)
Coal fly-ash-prepared zeolite 4A	Cu^{2+}	50.45	Hui et al. (2005)
	Co^{2+}	13.72	Hui et al. (2005)
Commercial zeolite 4A	Cu^{2+}	53.45	Hui et al. (2005)
	Co^{2+}	11.52	Hui et al. (2005)
Natural zeolite	Cu^{2+}	8.97	Erdem et al. (2004)
	Co^{2+}	14.39	Erdem et al. (2004)
Coal gangue-derived zeolite NaX	Cu^{2+}	45.05	This paper
	Co^{2+}	44.53	This paper

Conclusion

The present study shows that the coal gangue was successfully converted into zeolite NaX with a specific area of 676.02 m^2/g and wide pore size distribution. Batch experiments suggests that the coal gangue prepared zeolite NaX exhibits great affinity to metal ions such as Co^{2+} and Cu^{2+}. Such a process was strongly depends on the initial metal ion concentration and pH of the aqueous solution. Longer time was necessary to reach equilibrium at higher initial metal ion concentration than lower ones. Kinetic adsorption mechanism studies indicated that the mechanism of removal of Co^{2+} and Cu^{2+} by the synthesized zeolite NaX was controlled by surface adsorption, intra-particle diffusion, and film diffusion. Langmuir model demonstrates a higher correlation coefficient compared with Freundlich model for Co^{2+} and Cu^{2+}, signifying monolayer coverage of active sites on the surface of the zeolite NaX. The adsorption capacity determined from Langmuir model was 44.53 and 45.05 mg/g for Co^{2+} and Cu^{2+}, respectively. Temkin and Dubinin–Radushkevich models indicate that the adsorption of Co^{2+} and Cu^{2+} on the synthesized zeolite NaX is a physical process. Above findings suggests that coal gangue-derived zeolite NaX can be used as an alternative economical adsorbent for metal ions removal.

References

Abdelnaeim MY, El Sherif IY, Attia AA, Fathy NA, El-Shahat MF (2016) Impact of chemical activation on the adsorption performance of common reed towards Cu(II) and Cd(II). Int J Miner Process 157:80–88

Apiratikul R, Pavasant P (2008) Sorption of Cu^{2+}, Cd^{2+}, and Pb^{2+} using synthesized zeolite from coal fly ash. Chem Eng J 144:245–258

Argun ME (2008) Use of clinoptilolite for the removal of nickel ions from water: kinetics and thermodynamics. J Hazard Mater 150:587–595

Arivoli S, Ravichandran T (2013) Adsorption of Rhodamine-B from aqueous solution by activated calcite powder studies on equilibrium isotherm, kinetics and thermodynamics. Int J Pollut Abat Technol 2:6–12

Bailey SE, Olin TJ, Bricka RM, Adrian DD (1999) A review of potentially low-cost sorbents for heavy metals. Water Res 33:2469–2479

Baker HM, Massadeh AM, Younes HA (2009) Natural Jordanian zeolite: removal of heavy metal ions from water samples using column and batch methods. Environ Monit Assess 157:319–330

Bradl HB (2004) Adsorption of heavy metal ions on soils and soils constituents. J Colloid Interface Sci 277:1–18

Chaudhry SA, Khan TA, Ali I (2017a) Zirconium oxide-coated sand based batch and column adsorptive removal of arsenic from water: isotherm, kinetic and thermodynamic studies. Egypt J Pet 26:553–563

Chaudhry SA, Zaidi Z, Siddiqui SI (2017b) Isotherm, kinetic and thermodynamics of arsenic adsorption onto iron-zirconium binary oxide-coated sand (IZBOCS): modeling and process optimization. J Mol Liq 229:230–240

Chen J, Lu X (2017) Synthesis and characterization of zeolites NaA and NaX from coal gangue. J Mater Cycles Waste Manag. doi:10.1007/s10163-017-0605-5

Covarrubias C, Arriagada R, Yáñez J, García R, Angélica M, Barros SD, Arroyo P, Sousa-Aguiar EF (2005) Removal of chromium (III) from tannery effluents, using a system of packed columns of zeolite and activated carbon. J Chem Technol Biotechnol 80:899–908

Dabrowski A, Hubicki Z, Podkościelny P, Robens E (2004) Selective removal of the heavy metal ions from waters and industrial wastewaters by ion-exchange method. Chemosphere 56:91–106

El-Bahy SM, El-Bahy ZM (2016) Synthesis and characterization of a new iminodiacetate chelating resin for removal of toxic heavy metal ions from aqueous solution by batch and fixed bed column methods. Korean J Chem Eng 33:2492–2501

Erdem E, Karapinar N, Donat R (2004) The removal of heavy metal cations by natural zeolites. J Colloid Interface Sci 280:309–314

Göde F, Öztürk N, Sert Y, Bahçeli S (2010) Adsorption of Cr(VI) from aqueous solutions onto raw and acid-activated Reşadiye and Hançılı clays. Spectrosc Lett Int J Rapid Commun 43:68–78

Ho YS, McKay G (1999) Pseudo-second order model for sorption processes. Process Biochem 34:451–465

Huang Y, Wang K, Dong D, Li D, Hill MR, Hill AJ, Wang H (2010) Synthesis of hierarchical porous zeolite NaY particles with controllable particle sizes. Microporous Mesoporous Mater 127:167–175

Hui KS, Chao CYH, Kot SC (2005) Removal of mixed heavy metal ions in wastewater by zeolite 4A and residual products from recycled coal fly ash. J Hazard Mater 127:89–101

Iannazzo D, Pistone A, Ziccarelli I, Espro C, Galvagno S, Giofre SV, Romeo R, Cicero N, Bua GD, Lanza G, Legnani L, Chiacchio MA (2017) Removal of heavy metal ions from wastewater using dendrimer-functionalized multi-walled carbon nanotubes. Environ Sci Pollut Res 24:14735–14747

Kumar R, Chawla J (2014) Removal of cadmium ion from water/wastewater by nano-metal oxides: a review. Water Qual Expo Health 5:215–226

Lei B, Hu F, Yang X (2009) Synthesis of zeolite A from coal gangue. Deterg Cosmet 9:36–38 **(in Chinese)**

Lin CY, Yang DH (2002) Removal of pollutants from wastewater by coal bottom ash. J Environ Sci Health Part A 37:1509–1522

Moghadam MR, Nasirizadeh N, Dashti Z, Babanezhad E (2013) Removal of Fe(II) from aqueous solution using pomegranate peel carbon: equilibrium and kinetic studies. Int J Ind Chem 4:1–6

Padervand M, Gholami MR (2013) Removal of toxic heavy metal ions from waste water by functionalized magnetic core–zeolitic shell nanocomposites as adsorbents. Environ Sci Pollut Res 20:3900–3909

Petrovič A, Simonič M (2016) Removal of heavy metal ions from drinking water by alginate-immobilised *Chlorella sorokiniana*. Int J Environ Sci Technol 13:1761–1780

Qian T, Li J (2015) Synthesis of Na-A zeolite from coal gangue with the in situ crystallization technique. Adv Power Technol 26:98–104

Rahimi E, Mohaghegh N (2016) Removal of toxic metal ions from sungun acid rock drainage using mordenite zeolite, grapheme nanosheets, and a novel metal–organic framework. Mine Water Environ 35:18–28

Rivera-Utrilla J, Sánchez-Polo M (2003) Adsorption of Cr(III) on ozonised activated carbon. Importance of Cπ—cation interactions. Water Res 37:3335–3340

Salam MA (2013) Removal of heavy metal ions from aqueous solutions with multi-walled carbon nanotubes: kinetic and thermodynamic studies. Int J Environ Sci Technol 10:677–688

Srividya K, Mohanty K (2009) Biosorption of hexavalent chromium from aqueous solutions by *Catla catla* scales: equilibrium and kinetics studies. Chem Eng J 155:666–673

Tansel B, Sager J, Rector T, Garlang J, Strayer RF, Levine LF, Roberts M, Hummeick M, Bauer J (2006) Significance of hydrated radius and hydration shells on ionic permeability during nanofiltration in dead end and cross flow modes. Sep Purif Technol 51:40–47

Thamilarasu P, Karunakaran K (2013) Kinetic, equilibrium and thermodynamic studies on removal of Cr(VI) by activated carbon prepared from *Ricinus commuis* seed shell. Can J Chem Eng 91:9–18

Turan M, Mart U, Yüksel B, Çelik MS (2005) Lead removal in fixed-bed columns by zeolite and sepiolite. Chemosphere 60:1487–1492

Xu W, Li LY, Grace JR (2010) Zinc removal from acid rock drainage by clinoptilolite in a slurry bubble column. Appl Clay Sci 50:158–163

Yuan Q, Li N, Chi Y, Geng W, Yan W, Zhao Y, Li X, Dong B (2013) Effect of large pore size of multifunctional mesoporous microsphere on removal of heavy metal ions. J Hazard Mater 254–255:157–165

Zhang Z, Wang W, Yang XY, Hu QX, Li YF (2008) Preparation of 4A zeolite from coal gangue through a alkali fusion method. China Surfactant Deterg Cosmet 5:294–297 **(in Chinese)**

Zhao Y, Zhang B, Zhang X, Wang J, Liu J, Chen R (2010) Preparation of highly ordered cubic NaA zeolite from halloysite mineral for adsorption of ammonium ions. J Hazard Mater 178:658–664